Measuring elastic parameters of cells by micropipette aspiration: application to lymphocytes

Gustavo Esteban-Manzanares[1,2], Blanca González-Bermúdez[1,2], Julia Cruces[3], Mónica De la Fuente[3], Gustavo V. Guinea[1,2], José Pérez-Rigueiro[1,2], Manuel Elices[1,2], Gustavo R. Plaza[1,2]

[1] Center for Biomedical Technology. Universidad Politécnica de Madrid, 28223 Pozuelo de Alarcón, Spain.

[2] Departamento de Ciencia de Materiales, ETSI de Caminos, Canales y Puertos. Universidad Politécnica de Madrid, 28040 Madrid, Spain.

[3] Departamento de Fisiología Animal II, Facultad de Biología, Universidad Complutense de Madrid, E-28040, Madrid, Spain.

ABSTRACT

Mechanical deformability of cells is an important property for their function and in development, and a useful marker of cell state. Moreover measuring mechanical properties of cells has been proven useful in preclinical studies and in clinical practice. We provide here a method to measure the two parameters, elastic modulus and Poisson coefficient, of the cellular material under the approximation of homogeneous isotropic linear elasticity. The proposed method is based on the analysis of micropipette aspiration experiments. We show the successful application of this procedure to measure the elastic parameters of lymphocytes, for which the mechanical properties depend on the activation state, and their measurement would be useful in clinical studies and clinical practice. The method will be valuable to be implemented in future technologies, based on the micropipette aspiration technique, for the automated measurement of mechanical properties of cells.

Keywords

Cell deformability, mechanical properties of cells, micropipette aspiration, elastic parameters

INTRODUCTION

Numerous works have stablished that the mechanical properties of cells are useful markers of cell state. Furthermore, the deformability of cells is a promising immune-label-free biomarker for various disease processes and changes in cell state, and is based on the associated cytoskeletal and nuclear changes (1, 2).

Mechanical deformability of the eukaryotic cell is a key property, important in cell migration. In particular, deformability plays a vital role in the case of blood and immune-system cells, since their activity is dependent on the ability to flow through narrow channels. In this field, stiffening of red blood cells by malaria parasite complicates the blood flow, while migration of cancer cells is facilitated by their higher deformability (3). In stem cells deformability plays a major role in their ability to migrate, which is crucial for tissue regeneration (4, 5). As an example, we showed in a previous work that a higher deformability of mesenchymal stem cells (cardiac mesoangioblasts) was related to improved behavior in tissue regeneration (6). Additionally mechanical cues are determinant for the fate of stem cells (7, 8). In the case of immune-system cells, previous works studied the deformability of neutrophils and monocytes showing how this property may change upon stimulation with chemokines associated with infection or stress (9-11). This importance of the mechanical properties justifies the interest in developing simple procedures to measure the mechanical properties of cells in an automatic or nearly-automatic manner. Some of the procedures currently under development are based on the micropipette aspiration technique (1), and we propose here a methodology to compute the elastic parameters, i.e. elastic modulus and Poisson coefficient, in the frame of the first-approximation description of the cell as a homogeneous linear elastic material.

The mechanical properties of cells may be studied using different techniques (12, 13), each with a different method to apply a mechanical deformation and measure the corresponding force. Techniques such as indentation by atomic force microscopy or magnetic beads twisting permit to deform a small region of the cell and therefore to measure the local properties. In a different way, micropipette aspiration allows applying large deformations to the whole cell by suction with a microcapillary, typically called micropipette. Micropipette aspiration is one of the easiest techniques in the field, due to the simplicity of the experimental device and the way the tests are carried out, although the analysis of the measurements is more complicated and requires digital image processing.

Currently there is a palette of available techniques to measure mechanical properties of cells, based on different physical principles. (i) Atomic force microscopy is based on the deflection of a cantilever with a tip indented into a specific location of a cell and usually is applied to measurements on adherent cells (14), though it can be used for non-adherent cells if fixed on a substrate (15). (ii) Micropipette aspiration technique consists of aspirating the cell by a microcapillary and analyzing the aspirated length produced by a suction pressure (16), allowing computing elastic or viscoelastic parameters for low deformations under the assumption of incompressibility (17) or the cytoplasm apparent viscosity for large deformation (18). In this article we propose to add a second dimensional measurement, which allows measuring two elastic parameters, as explained below. Micropipette aspiration is usually applied to nonadherent cells, with largely spherical symmetry (19), and can be also applied to suspended adherent cells (18). (iii)

In magnetic twisting rheology (20), the response of a cell-attached magnetic bead is probed in response to an external magnetic field.

Various promising approaches are being developed with the aim of performing measurements of mechanical properties of very large numbers of cells. (iv) The optical stretching technique uses optical gradient forces to stretch the cell (21). An important limitation of this technique is the heating of the cells. (v) Deformability cytometry is a hydrodynamic approach, in which cells are deformed by deceleration at the stagnation point of fast extensional flow (2). (vi) Another group of automatic-measurement techniques consists of measuring the transit time as cells pass through flow constrictions, single or multiple pores (22). (vii) The automatic measurement of properties based on the micropipette aspiration technique is closely related to the previous group, using a cylindrical microchannel, and allowing applying the available models for this technique. Below we describe the methodology we have developed, allowing estimating two elastic parameters.

At low deformations, the cell behaves like a solid (23, 24) and analyzing its mechanical properties allows identifying the role played by different components in the cells (23, 25, 26), complementing the studies of the internal components, in particular the cytoskeleton (27).

In this context, our aim was to develop a methodology to measure the elastic modulus and the Poisson coefficient by using micropipette aspiration. Importantly, the structural nonlinearity of the problem is carefully considered. We explain here the proposed two-step procedure, analyzing in detail the mechanical model. Using this simple procedure, we estimated the elastic parameters of lymphocytes, evaluating the application of the simplified methodology. Characterizing their mechanical properties will be of interest in clinical and pre-clinical applications.

We consider that the methodology described in this work will facilitate to carry out large-scale studies of the relation between physicochemical cues or diseases and the mechanical behavior of cells. Systematic studies of the deformability of lymphocytes could provide new insights in studies of immunosenescence, biocompatibility and infection.

MATERIALS AND METHODS

Finite elements model

The commercial finite element software Abaqus (Dassault Systèmes Simulia Corp., USA) has been used to perform the finite element analysis. We have built an axisymmetric model (see figure 1) of a spherical cell, using Abaqus preprocessor. The mesh of the spherical cell contains four- and three-nodes elements (CAX4H, CAX3H), with first-orden interpolation and hybrid formulation. The mesh was finer on the zone close to the contact with the rigid surface of the microcapillary. The cell material is elastic. The surface of the microcapillary is modeled as a rigid surface and contains a filet radius $R_f = R_p/20$ (see figure 1, read the justification in the section on the results of the model). In the model, lengths and displacements are measured in units of the internal radius of the micropipette, R_p, and stress in units of the elastic modulus E.

The contact between the spherical cell and the surface of the microcapillary is frictionless. The radial displacement is impeded for the nodes on the axis of symmetry. The differential pressure ΔP is applied on the surface of the cell placed inside the micropipette.

We studied the convergence of the calculations by progressively doubling the number or nodes on the boundaries, guarantying that convergence was reached.

Cells

We have used female ICR-CD1, *Mus musculus*, mice (Janvier S.A.S., Le Genest-St-Isle, France). Animals were treated according to the guidelines of the European Community Council Directives 1201/2005 EEC and the experimental protocol was approved by the Animal Ethics Committee of the Universidad Complutense de Madrid (Spain). Peritoneal leukocytes were obtained from mice, by injecting intraperitoneally 3 ml of sterile Hank's solution, previously tempered at 37ºC. After massaging the abdomen, 80 % of the injected volume was recovered. Non-adherent lymphocytes were isolated by incubating the peritoneal leukocyte population at 37 ºC in a humidified atmosphere of 5% CO_2, for 45 minutes, using migratory inhibitory factor plates (Kartell, Noviglio, Italy). The supernatants were collected using a Pasteur pipette. Starting lymphocyte concentration was of the order of 10^5 cell/ml. Cells were maintained at 4ºC until the micropipette aspiration experiments.

Micropipette aspiration experiments

The experimental technique for the micropipette-aspiration experiments is graphically sketched in Figure 6. Micropipette aspiration experiments were conducted in a custom-built device (6, 18) similar to those described previously (28), using microcapillaries with a nominal internal diameter of 5 µm. The suspension of cells (~0.25 mL) was deposited on a cover-glass plate placed in an optical Leica DMI3000B inverted microscope. The microcapillary was connected to a distilled water reservoir and the differential pressure was applied by a difference in height of the reservoir with respect to the cells dispersion. The differential pressure ΔP was increased at a rate of 0.5 Pa/s. The aspiration process was studied by time-lapse imaging. The images were analyzed with the software imageJ (http://rsb.info.nih.gov/ij), to measure the internal radius of the micropipette R_p, the initial radius of the cell R_c, the aspirated length L_p and the transversal diameter D_t (see figure 1).

MODEL

Linear elasticity

The micropipette aspiration technique has been used during the last decades in mechanical studies of individual cells. Several mechanical models have been developed, including models appropriate to measure the shear rigidity of the red-blood-cell membrane (29), the cortical tension for a cell considered a spherical drop of negligibly-viscous fluid with a contractile cortex (19) or the apparent viscosity of the cell during its large-deformation flow into the micropipette (18, 30, 31).

For small deformation the cell behavior may be described as solid-like (23, 24), and the simplest approach is to describe the cell as a homogeneous, isotropous and elastic solid. Theret et al. obtained an analytical equation to compute the elastic modulus by modeling the cell as a homogeneous, isotropous, non-compressible and elastic half-space (32). Zhou et al. developed a numerical model for a spherical cell of non-compressible neo-Hookean material, fitting an equation that allows computing the elastic modulus of the cell (33). A linearized version for small deformation was obtained later (17). Li and Chen used a numerical model to develop an equation for a homogeneous, isotropous, and linear-elastic spherical cell (34). With their equation it was not possible to calculate the two parameters of the material, i.e. the elastic modulus and the Poisson's coefficient. Besides, the structural non-linearity of the problem, due to the contact and slipping between the cell and the surface of the microcapillary, was obviated in that interesting work.

Here, to develop a straightforward method to characterize the cell in small deformation, the cell is described as a homogeneous, isotropous, and linear-elastic sphere.

Kinematic variables

In the previous models the only directly-measurable kinematic variable utilized in the equations is the distance advanced by the front of the cell, L_p (see figure 1). This election limits the possibilities of computing mechanical parameters.

Figure 1b shows that during the aspiration of the cell, there is a radial displacement of the surface of the cell. Therefore, it is possible to compute the transversal contraction of the cell, ΔD_t, (see figure 1b) due to the aspiration process. Using the two kinematical variables, L_p and ΔD_t, allows estimating the two parameters of the linear elastic material, the elastic modulus E and the Poisson's coefficient ν, as explained below.

Structural non-linearity due to the contact between cell and the micropipette

Even for a linear elastic material and for small deformation, the aspiration of the cell constitutes a case of structural non-linearity due to the contact (35) and also to the slipping between the deformable cell and the rigid surface of the micropipette.

COMPUTED ASPIRATION CURVES

The two geometric parameters in the aspiration analysis are the nondimensional radius of the cell R_c/R_p and filet radius R_f/R_p. Using the nondimensional aspiration pressure $\Delta P/E$, the third parameter independent parameter is the Poisson's coefficient ν. In the aspiration experiments, the relative radius of the cell R_c/R_p is easily optically measured, the Poisson's coefficient is one of the parameters to be estimated and, however, the filet radius cannot be measured optically because of its small size (see for instance Figure 6a below). Moreover, the filet radius is not considered in the equations obtained in the previous works (32-34).

Figures 2a and 2c show respectively the curves for the nondimensional pressure $\Delta P/E$ and transversal contraction $\Delta D_t/R_p$, versus the nondimensional aspirated length L_p/R_p, for 5 values of the Poisson's coefficient ν and three values of the nondimensional filet radius. In the figure the radius of the cell is kept constant, R_c/R_p=1.15. Apart from the obvious importance of the cell radius, the figure shows that both the Poisson's

coefficient and the filet radius have an important influence on the curves. Therefore, a priori, it could be necessary to consider the filet radius to compute the elastic parameters of the aspirated cell.

The value of the filet radius is important because it is related to the sharpness of the contact area between the cell and the microcapillary. Additionally, the contact area depends also on the roughness of the cell. Furthermore, considering a very small value for the filet radius, as measured (for instance by electron microscopy) in the microcapillary, would produce an erroneous result, since the contact area would be larger than computed due to the ruffles and microvilli of the cell. Therefore, the value of the filet radius used in the calculations must be in agreement with the roughness of the cell. As explained in the next lines, it is possible to estimate reasonably a practical value $R_f = R_p/20$, which has been used in the calculations. On one side, in the micropipettes typically used in aspiration experiments, with internal radius R_p between 5 and 10 μm, the filet radius R_f (see Figure 1b) is very tiny and clearly smaller than the resolution in an optical microscope (see for instance Figure 6a below). On the other side, the value of R_f used in the model must be at least of the order of the roughness of the cell surface, due to the ruffles and microvilli. For the small blood cells typically tested with 5-μm micropipettes, the cell-surface roughness is of the order of 0.1 μm (36), and for larger suspended cells that can be aspirated with a micropipette of $R_p \sim 10$ μm the roughness is approximately twice larger (37). This reasoning justifies using $R_f \sim R_p/20$.

Following the previous reasoning, we propose in this work to compute the elastic parameters of the cell by assuming $R_f/R_p = 0.05$. The elastic modulus and Poisson's coefficient are labelled, for that reason, $E_{0.05}$ and $\nu_{0.05}$.

Comparison with previous works

Three previous works analyzed the aspiration process considering a cell of homogeneous isotropic elastic material. In all the three works, the cell was assumed incompressible, i.e. with a Poisson's coefficient $\nu = 0.5$ if it is the linear elastic. Theret et al. modeled the cell as a linear elastic half-space (32). In their analytic solution, the nonlinearities due to the contact of two solids and the sliding between them were not considered. Zhou et al. considered a neo-Hookean material and took into account the nonlinearities (33). By fitting their numerical results, they obtained an equation relating pressure, aspirated length, geometrical constants and elastic modulus. Li and Chen analyzed the problem modeling the cell as a linear elastic material (34). In their numerical study, the effect of the nonlinearities was not analyzed. They also proposed an equation obtained by fitting the numerical results. The equations developed in those three works can be used to estimate the elastic modulus of the cell from the experimental curves differential pressure vs. aspirated length, providing different results.

One important limitation to fit the curves differential pressure vs. aspirated length is the nonlinearity of the problem, which may produce different results depending on the range of values for which the fitting is performed. To compare the previous models and our results (with $\nu = 0.5$ and $R_f/Rp = 0.05$), we have computed the initial slope (tangent at origin) of the curves $\Delta P/E$ vs. L_p/R_p for three different ranges of values. The reason for using different ranges is to estimate on one hand the initial slope for very small deformation ($0 < L_p/R_p < 0.001$) and on the other hand the apparent initial slope obtained by fitting the curve in a range of realistically measurable displacements in an

aspiration experiment ($0 < L_p/R_p < 0.3$). An intermediate range is also included. The different values for the initial slope are shown in Figure 3.

Figure 3 shows firstly the inaccuracy of the equation developed by Theret et al. due to its limitations (finite size of the cell and nonlinearities not included in the model). At very large values of R_c/R_p, the slope provided by that equation coincides with the initial slope in our calculations (by fitting the curves in the range of very small deformations, $L_p/R_p < 0.001$). The figure shows also that the initial slope provided by Zhou et al.'s equation is similar (in its range of validity) to the initial slope estimated in this work when fitting the curves in the range of moderate displacements, L_p/R_p up to 0.1-0.3. Finally, Li and Chen's equation gives an initial slope similar to the initial slope in our curves ($L_p/R_p < 0.001$) for cell sizes relatively large, $R_c/R_p \geq 2.3$.

The figure also shows that an equation that provides the initial slope ($L_p/R_p < 0.001$) of the curve $\Delta P/E$ vs. L_p/R_p is not of practical use because of the impossibility of measuring optically very small displacements of the front of the aspirated cell. The need to develop a procedure to estimate the elastic parameters in an aspiration experiment implies that a proposed equation should fit the curve $\Delta P/E$ vs. L_p/R_p in a range of displacements that can be realistically measured and we propose the range $0 < L_p/R_p < 0.3$. In the next paragraphs we describe the proposed procedure. Our model will provide similar results to Zhou et al.'s equation in its range of validity and when $\nu = 0.5$ (as shown in Figure 3).

PROPOSED PROCEDURE TO ASSESS THE ELASTIC PARAMETERS

Procedure to evaluate the Poisson coefficient

The relationship between transversal contraction ΔD_t and displacement of the cell front L_p as a function of the Poisson's coefficient ν has been studied to obtain an expression to evaluate ν. As an example, Figure 4a shows D_t/R_p versus L_p/R_p, as a function of ν, for a ratio between radius of the cell and radius of the pipette $R_c/R_p = 1.1$. We found that the curves can be conveniently fitted to the expression

$$\frac{\Delta D_t}{R_p} = m_1 \left(1 + \frac{L_p}{R_p}\right)^{m_2} \left(e^{m_3 \frac{L_p}{R_p}} - 1\right) \qquad (1)$$

The parameters m_1, m_2 and m_3 depend on the Poisson's coefficient and the radii ratio R_c/R_p. The slope of the curve at the origin is $m_0 = m_1 m_3$. We computed the slope m_0 for each curve, using equation 1 to fit the curve in the range $0 < L_p/R_p < 0.3$. We studied the slope at the origin as a function of ν and R_c/R_p, as shown in figure 4b, obtaining by fitting the following expression (surface also shown in figure 2b):

$$m_0 = \frac{1}{\alpha_1}\left[1 + \alpha_2 \frac{R_c}{R_p} + \alpha_3 \left(\frac{R_c}{R_p}\right)^2\right]\left[1 - \left(\frac{\nu_{0.05}}{\alpha_4}\right)^{\alpha_5}\right] \qquad (2)$$

where the numerical values of the constants are shown in Table 1. In practice, the Poisson's coefficient must be computed from the ratio R_c/R_p and from the parameter m_0 estimated from numerical results; from equation (2) its value would be

$$\nu_{0.05} = \alpha_4 \left\{ 1 - \alpha_1 m_0 \left[1 + \alpha_2 \frac{R_c}{R_p} + \alpha_3 \left(\frac{R_c}{R_p} \right)^2 \right]^{-1} \right\}^{1/\alpha_5} \qquad (3)$$

Therefore, equations (1) and (3) are useful to estimate the Poisson's coefficient from the experimental data of the kinematic variables, not needing to take into account the differential pressure ΔP during the experiment.

Procedure to evaluate the elastic modulus

Evaluating the elastic modulus of the cell during the experiment requires taking into account the differential pressure ΔP. As an example, figure 4c shows the curves differential pressure vs. displacement of the cell front L_p, for different values of ν and for the ratio $R_c/R_p = 1.1$. Each curve was fitted, in the range $0 < L_p/R_p < 0.3$, to the expression

$$\frac{\Delta P}{E} = n_1 \left(\frac{L_p}{R_p} \right) + n_2 \left(\frac{L_p}{R_p} \right)^2 \qquad (4)$$

where the parameters n_1 and n_2 depend, again, on the Poisson's coefficient and the radii ratio R_c/R_p. We studied this dependence for n_1, as shown in figure 4d, obtaining by fitting the following expression (surface also shown in figure 4d):

$$n_1 = \frac{1 + \beta_1 \nu_{0.05}{}^{\beta_2} + \beta_3 R_c/R_p}{1 + \beta_4 R_c/R_p} \qquad (5)$$

where the numerical values of the constants are shown in Table 2. The parameter n_1 can be calculated from the Poisson's coefficient, obtained previously, and the radii ratio R_c/R_p. Once it is known, the elastic modulus E can be estimated by fitting the experimental data of differential pressure ΔP vs the non-dimensional displacement of the front of the cell L_p/R_p, being the estimated modulus equal to the linear term divided by n_1 (directly from equation 4):

$$\Delta P = E n_1 \left(\frac{L_p}{R_p} \right) + E n_2 \left(\frac{L_p}{R_p} \right)^2 \qquad (6)$$

Practical procedure

Figure 5 summarizes the procedure to estimate both the Poisson's coefficient and the elastic modulus from the experimental data. The previous equations have been obtained for the range $1.1 < R_c/R_p < 1.5$, because for large cell sizes the relative transversal contraction D_t/R_p is too small in the regime of moderately small deformations.

APPLICATION TO ESTIMATE THE ELASTIC PARAMETERS OF LYMPHOCYTES

We applied the previous equations to estimate the elastic modulus and Poisson's coefficient of lymphocytes. In the experiments, we applied a ramp of differential pressure $d\Delta P/dt$ = 5 Pa/s as schematized in Figure 6c. We measured the displacements in the digital images to obtain $\Delta D_t/R_p$ and L_p/R_p at any time. As an example, figure 6d-e show the experimental values and the curves obtained by fitting the equations in the range $0 < L_p/R_p < 0.3$.

By analyzing automatically NN experiments with $1.1 < R_c/R_p < 1.5$, we obtained the values $\nu_{0.05}$ = _____ ± _____ and $E_{0.05}$ = _____ ± _____ Pa. These values are in agreement with _____

DISCUSSION

→ Importance of our method to compare mechanical parameters measured with different experimental techniques…

→ Importance of filet radius: importance of the shape in the "constrictions" technique: in that case the filet radius may be bigger and small differences in the shape may result in very different results…

CONCLUSIONS

The simple method described in this work could be extremely useful to establish mechanical differences between different cells types. The method will be appropriate to be implemented in experiments with the micropipette aspiration technique and in future automated versions, allowing testing large numbers of cells in short times.

Previous works…. . Here, we have shown the possibility of ….

The deformability of lymphocytes must be considered a key property in relation to their migration ability, which is fundamental for infection recovery. ….

Tables

α_1	α_2	α_3	α_4	α_5
0.9259	-1.194	0.3711	15.96	0.1671

Table 1. Numerical values of the constants of equations (2) and (3), obtained for the range $1.1 < R_c/R_p < 1.5$.

β_1	β_2	β_3	β_4
0.561	-0.943	0.447	5.40

Table 2. Numerical values of the constants of equation (5) , obtained for the range $1.1 < R_c/R_p < 1.5$.

Figures

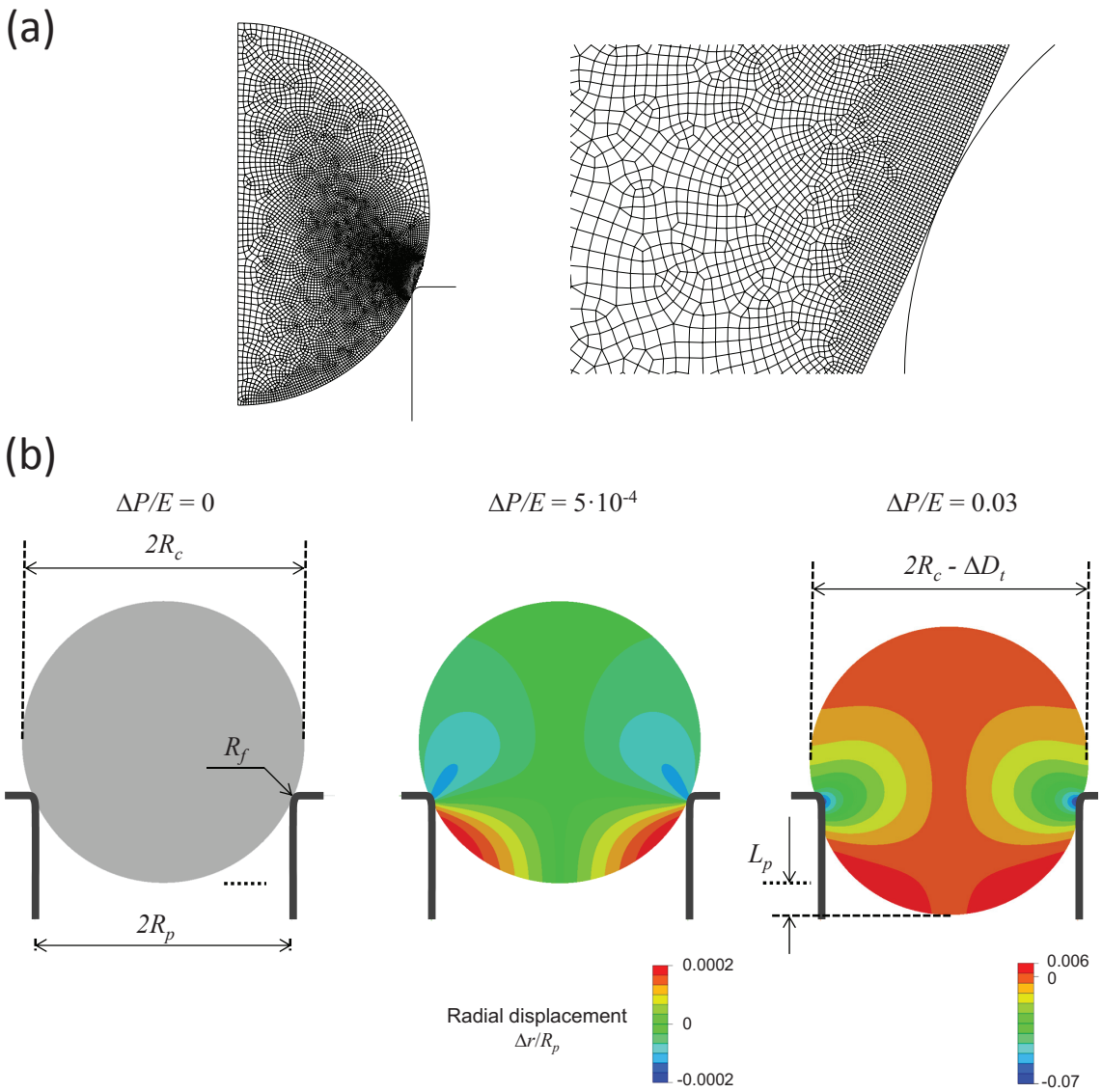

Figure 1. _____.

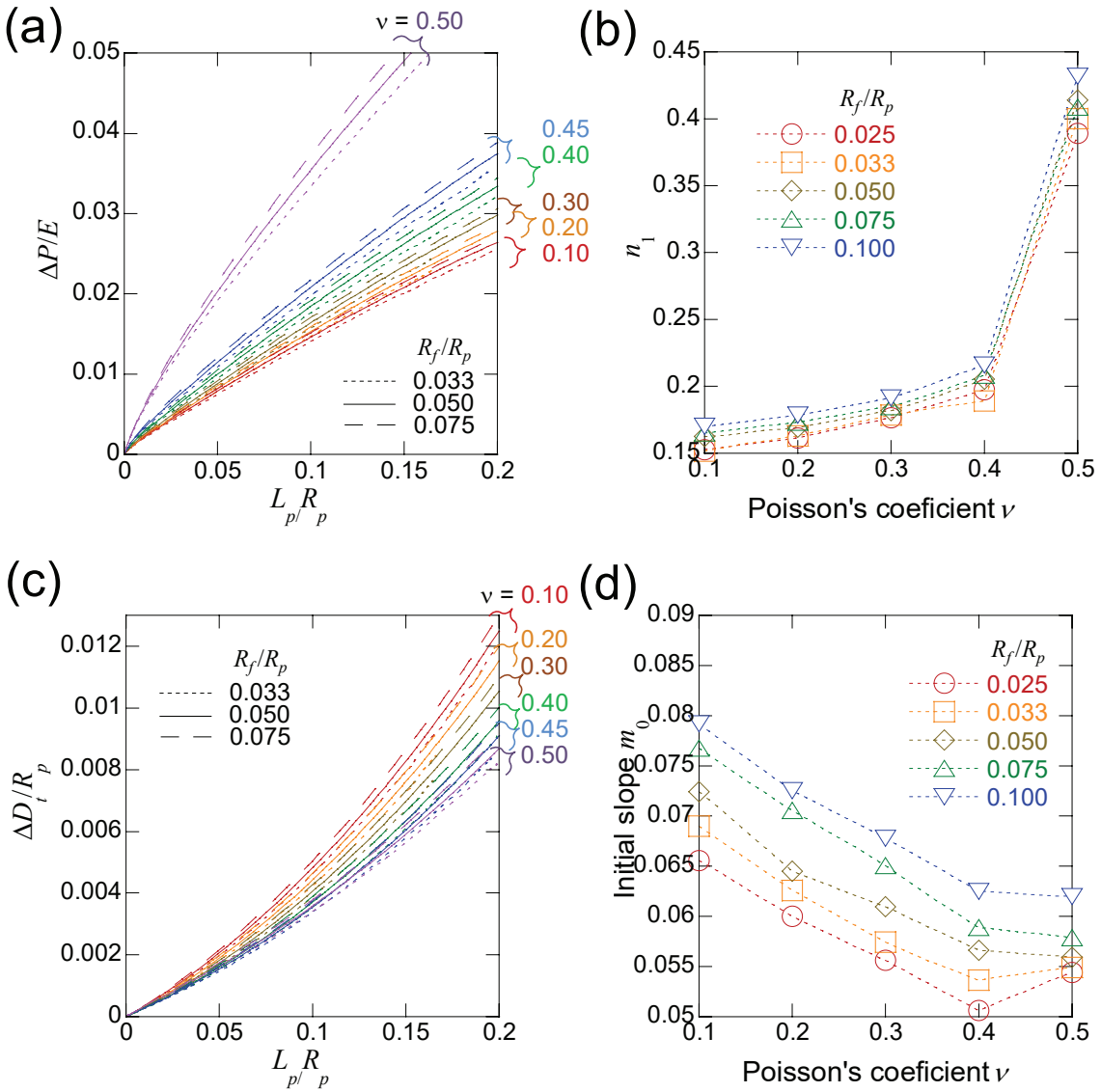

Figure 2. _____. The initial slopes in (b) and (d) were obtained by fitting the respectively the curves in (a) and (c) to the equations 4 and 1 in the range $0 < L_p/R_p < 0.3$.

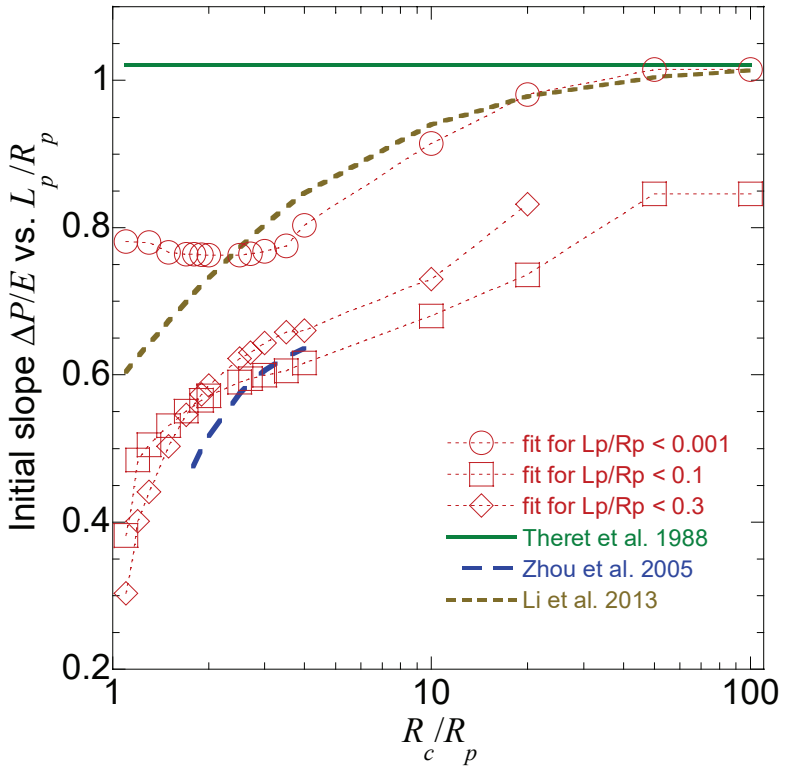

Figure 3. Initial slope of the curve $\Delta P/E$ vs. L_p/R_p in the equations developed by Theret et al. (32), Zhu et al. (17, 33), Li and Chen (34) and in the curves obtained in this work (with $\nu = 0.5$ and $R_f/Rp = 0.05$), obtained by fitting them to the equation 4, in the ranges $0 < L_p/R_p < 0.001$, $0 < L_p/R_p < 0.1$ and $0 < L_p/R_p < 0.3$. Zhu et al. developed their equation for the range $5/3 < R_c/R_p < 4$.

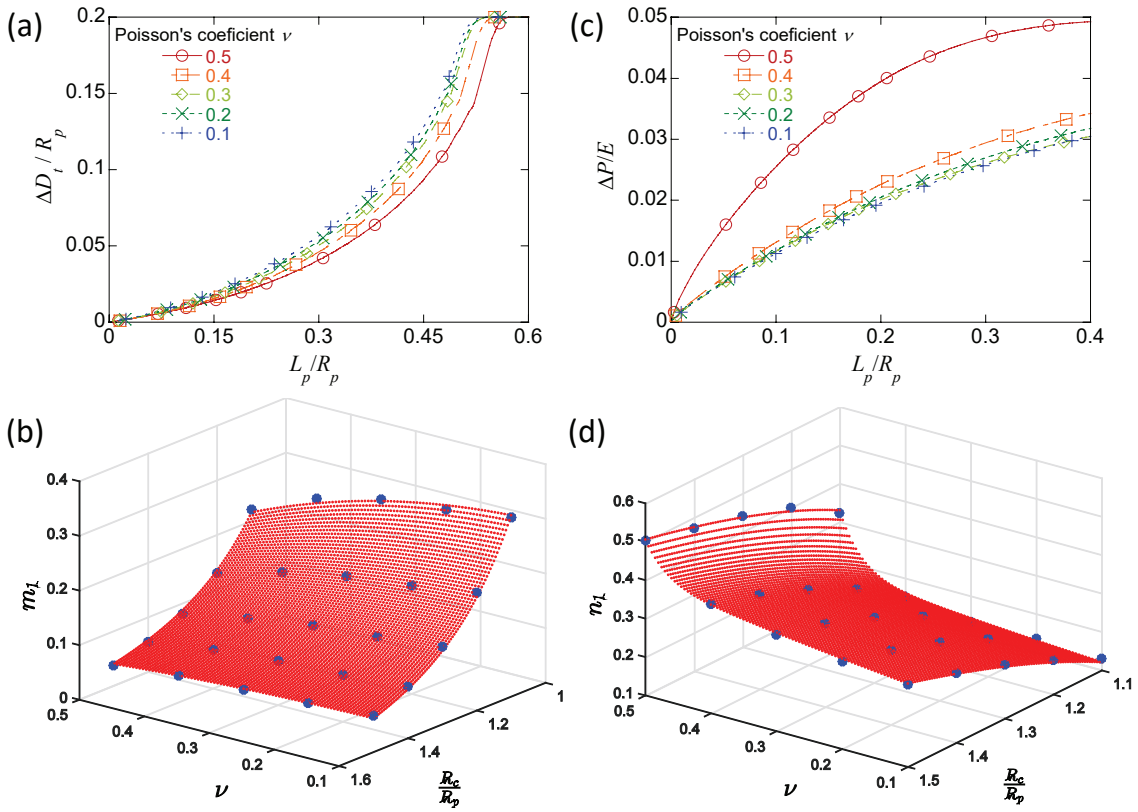
(a)
Poisson's coeficient ν
0.5
0.4
0.3
0.2
0.1
$\Delta D_t / R_p$
L_p / R_p
(c)
Poisson's coeficient ν
0.5
0.4
0.3
0.2
0.1
$\Delta P/E$
L_p / R_p
(b)
m_1
ν
$\frac{R_c}{R_p}$
(d)
n_1
ν
$\frac{R_c}{R_p}$

Figure 4. _____.

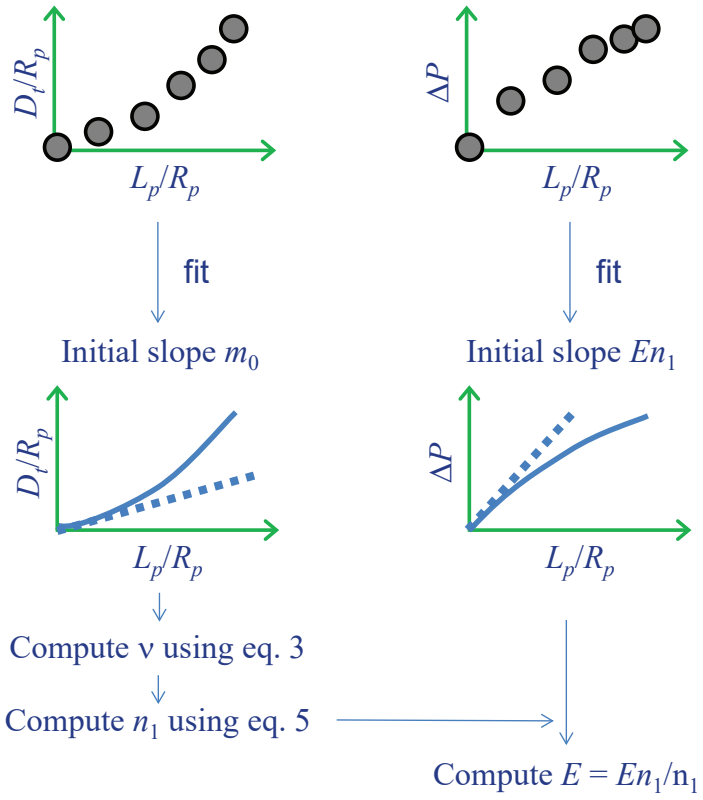
D_t/R_p
L_p/R_p
fit
Initial slope m_0
ΔP
L_p/R_p
fit
Initial slope En_1
D_t/R_p
L_p/R_p
ΔP
L_p/R_p
Compute ν using eq. 3
Compute n_1 using eq. 5
Compute $E = En_1/n_1$

Figure 5. _____.

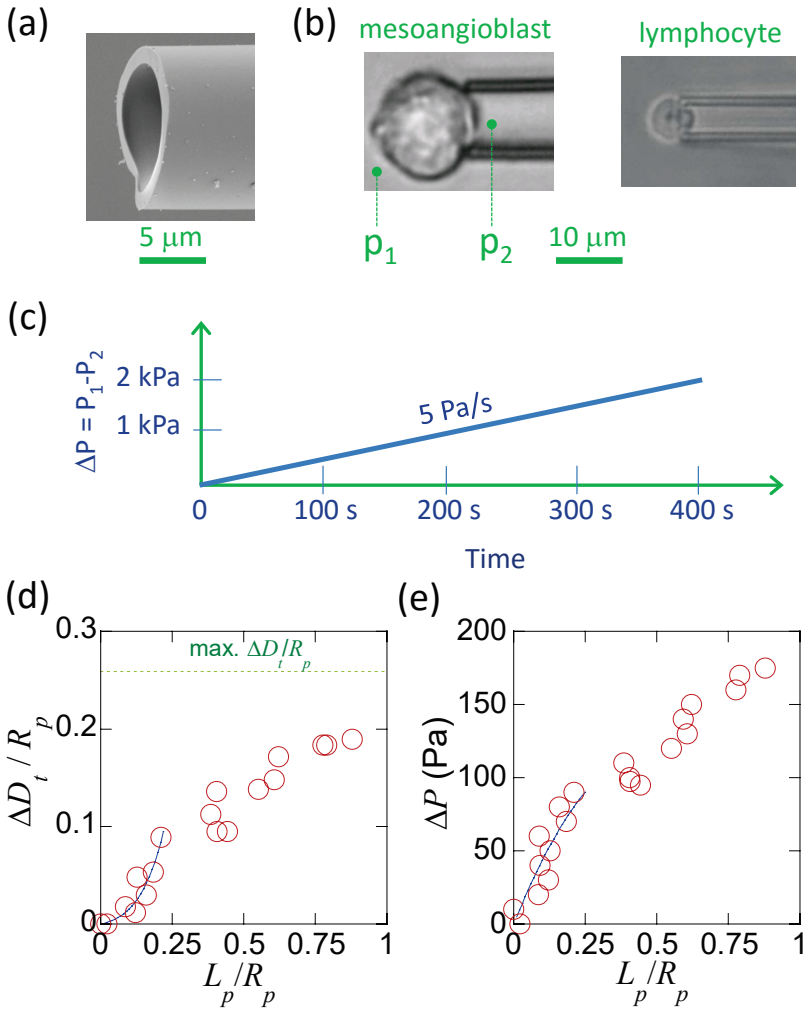

Figure 6. Micropipette aspiration experiments. (a) Electron microscope image of a glass microcapillary with an internal diameter $2R_p \sim 10$ µm. (b) Optical images obtained during aspirations experiments of a resuspended mesoangioblast ($2R_p \sim 10$ µm) and a lymphocyte ($2R_p \sim 5$ µm). (c) Scheme of the ramp of differential pressure applied during the experiments with lymphocytes analyzed in this work. (d-e) Experimental results and curves obtained by fitting for an aspiration experiment with a lymphocyte; the equations __ and __ were fitted in the range $0 < L_p/R_p < 0.3$; in this example, $R_c/R_p = 1.13$, $m_0 = 0.0610$, $\nu = 0.434$, $En_1 = 485$ Pa, $n_1 = 0.386$, $E = 1.26$ kPa.

References

Literature Cited

1. Di Carlo, D. 2012. A mechanical biomarker of cell state in medicine. J Lab Autom. 17, 32-42.

2. Gossett, D. R., H.T.K. Tse, S.A. Lee, Y. Ying, A.G. Lindgren, O.O. Yang, J. Rao, A.T. Clark and D. Di Carlo 2012. Hydrodynamic stretching of single cells for large population mechanical phenotyping. Proc. Natl. Acad. Sci. U. S. A. 109, 7630-7635.

3. Suresh, S., J. Spatz, J.P. Mills, A. Micoulet, M. Dao, C.T. Lim, M. Beil and T. Seufferlein 2005. Connections between single-cell biomechanics and human disease states: Gastrointestinal cancer and malaria. Acta Biomaterialia. 1, 15-30.

4. Lois, C. and A. Alvarezbuylla 1994. Long-distance neuronal migration in the adult mammalian brain. Science. 264, 1145-1148.

5. Ip, J. E., Y. Wu, J. Huang, L. Zhang, R.E. Pratt and V.J. Dzau 2007. Mesenchymal stem cells use integrin beta 1 not CXC chemokine receptor 4 for myocardial migration and engraftment. Mol. Biol. Cell. 18, 2873-2882.

6. Bernal, A., L.M. Perez, B. De Lucas, N.S. Martin, A. Kadow-Romacker, G. Plaza, K. Raum and B.G. Galvez 2015. Low-intensity pulsed ultrasound improves the functional properties of cardiac mesoangioblasts. Stem Cell Reviews. 11, 852-865.

7. Engler, A. J., S. Sen, H.L. Sweeney and D.E. Discher 2006. Matrix elasticity directs stem cell lineage specification. Cell. 126, 677-689.

8. Wang, N., J.D. Tytell and D.E. Ingber 2009. Mechanotransduction at a distance: Mechanically coupling the extracellular matrix with the nucleus. Nature Reviews Molecular Cell Biology. 10, 75-82.

9. Worthen, G. S., B. Schwab, E.L. Elson and G.P. Downey 1989. Mechanics of stimulated neutrophils - cell stiffening induces retention in capillaries. Science. 245, 183-186.

10. Nishino, M., H. Tanaka, H. Ogura, Y. Inoue, T. Koh, K. Fujita and H. Sugimoto 2005. Serial changes in leukcocyte deformability and whole blood rheology in patients with sepsis or trauma. Journal of Trauma-Injury Infection and Critical Care. 59, 1425-1431.

11. Poschl, J. M. B., P. Ruef and O. Linderkamp 2005. Deformability of passive and activated neutrophils in children with gram-negative septicemia. Scandinavian Journal of Clinical & Laboratory Investigation. 65, 333-339.

12. Rodriguez, M. L., P.J. McGarry and N.J. Sniadecki 2013. Review on cell mechanics: Experimental and modeling approaches. Appl. Mech. Rev. 65, 060801.

13. Bao, G. and S. Suresh 2003. Cell and molecular mechanics of biological materials. Nature Materials. 2, 715-725.

14. Haase, K. and A.E. Pelling 2015. Investigating cell mechanics with atomic force microscopy. Journal of the Royal Society Interface. 12, 20140970.

15. Daza, R., J. Cruces, M. Arroyo-Hernandez, N. Mari-Buye, M. De la Fuente, G.R. Plaza, M. Elices, J. Perez-Rigueiro and G.V. Guinea 2015. Topographical and mechanical characterization of living eukaryotic cells on opaque substrates: Development of a general procedure and its application to the study of non-adherent lymphocytes. Physical Biology. 12, 026005-026005.

16. Hochmuth, R. M. 2000. Micropipette aspiration of living cells. J. Biomech. 33, 15-22.

17. Plaza, G. R., T.Q.P. Uyeda, Z. Mirzaei and C.A. Simmons 2015. Study of the influence of actin-binding proteins using linear analyses of cell deformability. Soft Matter. 11, 5435-5446.

18. Plaza, G. R., N. Marí, B.G. Gálvez, A. Bernal, G.V. Guinea, R. Daza, J. Pérez-Rigueiro, C. Solanas and M. Elices 2014. Simple measurement of the apparent viscosity of a cell from only one picture: Application to cardiac stem cells. Physical Review E. 90, 052715.

19. Yeung, A. and E. Evans 1989. Cortical shell-liquid core model for passive flow of liquid-like spherical cells into micropipets. Biophys. J. 56, 139-149.

20. Butler, J. P. and S.M. Kelly 1998. A model for cytoplasmic rheology consistent with magnetic twisting cytometry. Biorheology. 35, 193-209.

21. Guck, J., S. Schinkinger, B. Lincoln, F. Wottawah, S. Ebert, M. Romeyke, D. Lenz, H.M. Erickson, R. Ananthakrishnan, D. Mitchell, J. Kas, S. Ulvick and C. Bilby 2005. Optical deformability as an inherent cell marker for testing malignant transformation and metastatic competence. Biophys. J. 88, 3689-3698.

22. Lange, J. R., J. Steinwachs, T. Kolb, L.A. Lautscham, I. Harder, G. Whyte and B. Fabry 2015. Microconstriction arrays for high-throughput quantitative measurements of cell mechanical properties. Biophysical Journal. 109, 26-34.

23. Trepat, X., L. Deng, S.S. An, D. Navajas, D.J. Tschumperlin, W.T. Gerthoffer, J.P. Butler and J.J. Fredberg 2007. Universal physical responses to stretch in the living cell. Nature. 447, 592-+.

24. Zhou, E. H., F.D. Martinez and J.J. Fredberg 2013. CELL RHEOLOGY mush rather than machine. Nature Materials. 12, 184-185.

25. Luo, T., K. Mohan, P.A. Iglesias and D.N. Robinson 2013. Molecular mechanisms of cellular mechanosensing. Nature Materials. 12, 1064-71.

26. Stewart, M. P., J. Helenius, Y. Toyoda, S.P. Ramanathan, D.J. Muller and A.A. Hyman 2011. Hydrostatic pressure and the actomyosin cortex drive mitotic cell rounding. Nature. 469, 226-230.

27. Plaza, G. R. and T.Q.P. Uyeda 2013. Contraction speed of the actomyosin cytoskeleton in the absence of the cell membrane. Soft Matter. 9, 4390-4400.

28. Trickey, W. R., G.M. Lee and F. Guilak 2000. Viscoelastic properties of chondrocytes from normal and osteoarthritic human cartilage. Journal of Orthopaedic Research. 18, 891-898.

29. EVANS, E. 1973. New membrane concept applied to analysis of fluid shear-deformed and micropipet-deformed red blood-cells. Biophys. J. 13, 941-954.

30. EVANS, E. and A. YEUNG 1989. Apparent viscosity and cortical tension of blood granulocytes determined by micropipet aspiration. Biophys. J. 56, 151-160.

31. Needham, D. and R.M. Hochmuth 1990. Rapid flow of passive neutrophils into a 4 mu-M pipette and measurement of cytoplasmic viscosity. Journal of Biomechanical Engineering-Transactions of the Asme. 112, 269-276.

32. Theret, D. P., M.J. Levesque, M. Sato, R.M. Nerem and L.T. Wheeler 1988. The application of a homogeneous half-space model in the analysis of endothelial-cell micropipette measurements. Journal of Biomechanical Engineering-Transactions of the Asme. 110, 190-199.

33. Zhou, E. H., C.T. Lim and S.T. Quek 2005. Finite element simulation of the micropipette aspiration of a living cell undergoing large viscoelastic deformation. Mechanics of Advanced Materials and Structures. 12, 501-512.

34. Li YongSheng and Chen WeiYi 2013. Finite element analysis of micropipette aspiration considering finite size and compressibility of cells. Science China-Physics Mechanics & Astronomy. 56, 2208-2215.

35. Alexandrov, V. M.andD. A. Pozharskii 2001. Three-dimensional contact problems. Kluwer Academic Publishers - Springer Netherlands,.

36. Majstoravich, S., J.Y. Zhang, S. Nicholson-Dykstra, S. Linder, W. Friedrich, K.A. Siminovitch and H.N. Higgs 2004. Lymphocyte microvilli are dynamic, actin-dependent structures that do not require wiskott-aldrich syndrome protein (WASp) for their morphology. Blood. 104, 1396-1403.

37. Friedmann, A., A. Hoess, A. Cismak and A. Heilmann 2011. Investigation of cell-substrate interactions by focused ion beam preparation and scanning electron microscopy. Acta Biomaterialia. 7, 2499-2507.